International Journal of Nanoelectronics and Materials
Volume 12, No. 2, Apr 2019 [237-250]

Analytical Approach Assisted Simulation Study of Si, SiGe, and InP based Bipolar Junction Transistors

M. R. Jena[1*], S. Mohapatra[1], A. K. Panda[2] and G. N. Dash[3]

[1]*Department of Electronics and Telecommunication Engineering, Veer Surendra Sai University of Technology, Burla, Sambalpur 768018, Odisha, India.*
[2]*Department of Electronics and Telecommunication Engineering, National Institute of Science and Technology, Berhampur 761008, Odisha, India.*
[3]*School of Physics, Sambalpur University, Sambalpur 768019, Odisha, India.*

Received 3 June 2018, Revised 12 September 2018, Accepted 16 November 2018

ABSTRACT

This paper presents a comparative study of Si, SiGe and InP based Bipolar Junction Transistors (BJT) with reference to their DC, AC, and RF characteristics. Double diffusion doping profile in each case is used to determine the common Figures of Merit (FOM) to assess their potentials for operation at high frequency. A theoretical analysis using Gummel-Poon model has been used to validate the data obtained from simulation using ATLAS module of SILVACO software tool. After validation of models, the three BJT's DC, AC and RF characteristics are evaluated and thereafter a comparative analysis has been carried out based on the important characteristics such as I–V behavior, frequency response, breakdown, maximum cutoff frequency, and minimum noise figure. It is observed that, with the same physical structure, InP BJT produced a high dc current gain (505) compared to a much lower value of the Si BJT (65). In contrast, the Si BJT provides higher cut-off frequency compared to the others.

Keywords: Silicon BJT, SiGe BJT, InP BJT, ATLAS Silvaco Tool, Semiconductors.

1. INTRODUCTION

Bipolar Junction Transistor (BJT) is one of the most widely explored three-terminal device seeking applications in both digital and analogue domains. With the advancement of technology, the device has undergone several transmutations aiming to achieve high transconductance, high speed, high cutoff frequency, and low noise figure. The Heterojunction Bipolar Transistor (HBT) has been able to fulfil these goals to some extent at the expense of complex manufacturing technology. Nonetheless, the fabrication of homojunction BJT has never relented and researchers continue to explore the device for its simple design and easy fabrication process compared to the HBT [1]. We believe that, with a judicious choice of the doping profile of the BJT, it may be possible to obtain device characteristics, which are at par with or better than those of the HBT [2]. For simplicity, it has become a common practice to consider the junctions as abrupt, which may be true for alloyed junctions in transistors. However, it is far from reality for junctions formed through diffusion or ion implantation techniques. Usually, in diffusion transistors, which has abrupt p-n junctions (with uniformly doped emitter, base, and collector regions), no drift field exists in the base region and the minority carriers injected from the emitter into the base only move by a diffusion process. On the other hand, drift transistors have a built-in electric field in which the minority carriers injected from the forward-biased emitter are accelerated towards the collector because of the sharp impurity gradient in the base region.

* Corresponding Author: *mrjena_etc@vssut.ac.in*

Consequently, a drift motion is superimposed over the normal diffusive motion of the minority carriers during their transit in the base region. Thus, the doping profile plays a major role in the characteristics of the BJT.

Therefore, this work proposes to undertake Gaussian doping profile for both the base-emitter (BE) and collector-base (CB) junctions. Such doping profile is not only realistic for diffused and ion-implanted junctions but also provides a drift field in the base region. Studies on BJT utilizing individual materials such as Si [1], SiGe [3] and InP [4] vastly available in the published literature unlike the comparative performance analysis of the three materials (Si, SiGe, and InP) that have similar structures and doping profile. Hence, this study will investigate the performance of the three materials.

By comparing with the previous experimental studies, this research has used simulation to understand the detailed physical process and operation of the BJTs [5]. While ATLAS module of SILVACO software was used as the main tool for the study, most of the simulation results were authenticated using analytical results from BJT theory. A comparative analysis of the three materials was carried out based on the common figures of merit such as I–V behavior, frequency response, maximum cutoff frequency, breakdown, and minimum noise figure. The rest of the paper is organized with device structure in Section 2, selection of models in Section 3, result and discussion in Section 4, and finally conclusion in Section 5.

2. DEVICE STRUCTURE

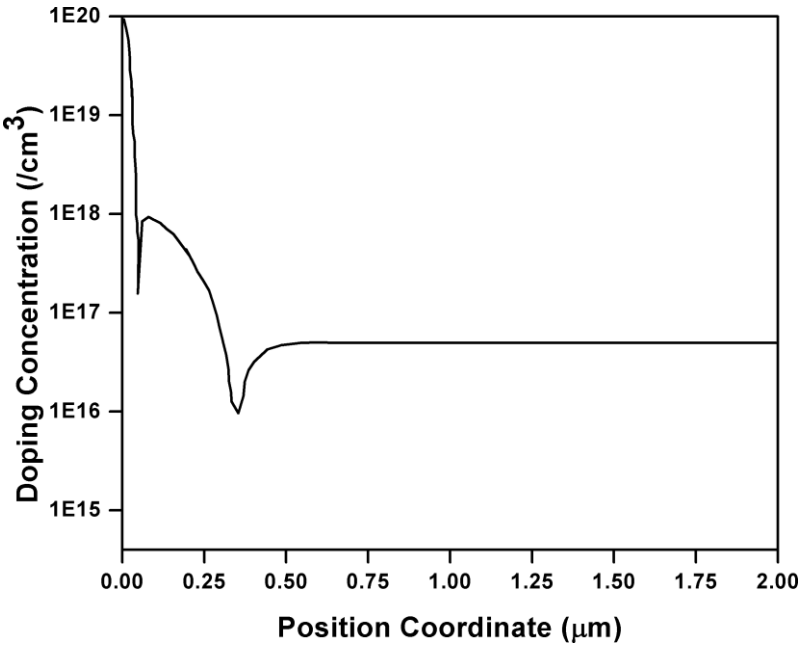

Figure 1. Doping profile of the proposed device.

The drift transistor that has been studied in this work has an n-type uniform concentration of $5\times10^{16}/cm^3$ in the collector region, a p-type Gaussian distribution of peak concentration $10^{18}/cm^3$ in the base, and an n-type Gaussian distribution of peak concentration $10^{20}/cm^3$ in the emitter region. The device structure has a total width of 2 μm; with the emitter, base and collector widths at 0.05 μm, 0.3 μm and 1.65 μm, respectively. The device is simulated using Silvaco T-CAD simulator with emitter area, A_E = 0.55 μm^2. The doping profile of the proposed device is shown in Figure 1. This is a double-diffused planar process in which p-type and n-type

diffusions are performed in succession on the same face of the wafer giving the impurity profile shown in Figure 1.

3. SELECTION OF MODELS

During device simulation, the model selection is important in order to get actual characteristics of the proposed device. Therefore, the models are selected based on the theoretically calculated value. Based on the physical geometry, the theoretical DC current gain, β is calculated shown below. Since we have considered a Gaussian distribution profile, the diffusion profile is represented by Equation (1):

$$C(\mathrm{x,t}) = \frac{Q_T}{\sqrt{\pi Dt}} \exp\left(\frac{-x^2}{4Dt}\right) \tag{1}$$

Where Q_T is the total impurity atoms per cm^2, D is the diffusivity constant of dopants (in cm^2/s), x is the distance (in cm), and t the diffusion time (in sec.). For this investigation, the Gummel-Poon model has been employed considering a non-uniform base doping and the presence of an electric field in the neutral base region. Therefore, there will be a drift component of the minority carrier current in the base in addition to the diffusion component. In npn transistor, the electron current in the base can be written as Equation (2) [6]:

$$I_n = qA\mu_n n(x)\mathrm{E} - qAD_n \frac{\partial n(x)}{\partial x} \tag{2}$$

The electric field in the base E can be estimated by assuming that the hole current in the base is negligible (and hence zero). This electric field is negative and moves from the collector to emitter in the base. Hence, it helps in the drifting of electrons from the emitter-end to the collector-end in the neutral base region. Substituting the value of the estimated electric field E into Equation (2), the total electron current passing through the base can be obtained using Equation (3):

$$I_n = -\frac{qAD_n}{p(\mathrm{x})} \frac{d}{dx} \{p(\mathrm{x})\mathrm{n}(\mathrm{x})\} \tag{3}$$

Integrating Equation (3) over the neutral base region and assuming that BE junction is forward biased and CB junction is reverse biased, then Equation (4) is obtained:

$$I_n = \frac{qAD_n n_i^2}{Q_B} \exp\left(\frac{qV_{BE}}{K_B T}\right) \tag{4}$$

Where,

$$Q_B = \int_0^{W_B} p(\mathrm{x})\mathrm{dx} \tag{5}$$

Q_B is referred to as the Base Gummel Number (BGN). In a straight forward extension of the above analysis for the emitter region, an expression for hole current in the emitter of a npn transistor can be obtained as:

$$I_p = \frac{qAD_p n_i^2}{Q_E} \exp\left(\frac{qV_{BE}}{K_B T}\right) \tag{6}$$

Where

$$Q_E = \int_0^{W_E} n(\mathrm{x})\,\mathrm{dx} \tag{7}$$

Q_E is defined as the Emitter Gummel Number (EGN). The integration is performed over the neutral region of emitter extending from 0 to W_E.

Let $N_{dE}(x)$ and $N_{aB}(x)$ be the doping distributions in the emitter and base respectively. Then the Gummel Numbers can be evaluated by assuming complete ionization of dopants given by:

$$Q_B = \int_0^{W_B} \mathrm{p}(\mathrm{x})\mathrm{dx} = \int_0^{W_B} \mathrm{N}_{aB}(\mathrm{x})\mathrm{dx} \tag{8}$$

$$Q_E = \int_0^{W_E} \mathrm{n}(\mathrm{x})\mathrm{dx} = \int_0^{W_E} \mathrm{N}_{dE}(\mathrm{x})\mathrm{dx} \tag{9}$$

The neutral base and emitter widths of bipolar junction transistors considered in this work are determined as the width where the value of electric field is approximately zero (a three order less in comparison to the peak electric field is set as the criterion for zero). The electric field distributions of the devices are extracted from the plot. The neutral widths of base and emitter region are determined from the web plot digitizer using the zero electric field criterion set above. The transistor β is obtained as:

$$\beta = \frac{Q_E}{Q_B} \tag{10}$$

The model developed above is now used to determine the Gummel numbers. The base and emitter Gummel numbers have been calculated analytically by performing the integrations [Eq. (8) and (9) respectively] of the dopant profile in the neutral base and emitter regions.

In this computation, we have considered concentration dependent mobility model, the parallel electric field dependence mobility model, concentration dependent recombination model, Auger recombination model, and band-gap narrowing model in each case of the BJTs. The concentration dependent mobility model is doping versus mobility table valid for 300K. The parallel electric field dependent mobility model is used to model any type of velocity saturation effect in the devices and the remaining models are used to account for the generation and recombination mechanisms inside the devices. For theoretical calculations of the Gummel numbers, the diffused junctions were approximated by exponential distributions of the form [7, 8]:

$$N(\mathrm{x}) = \mathrm{N}_0 \exp\left(-\frac{X}{\lambda}\right) - N_B \tag{11}$$

Where N_0 is the impurity concentration at the surface, N_B is the background concentration in the starting sample, *x* is the distance from the surface into the semiconductor, and λ is the characteristic length. The λ values for the approximated exponential distributions are obtained by the process of curve fitting from a MATLAB software. Finally, the following Gummel numbers and the resultant DC gains were obtained for the three materials based BJTs:

$$\beta = \frac{Q_E}{Q_B} = \frac{8.8929 \times 10^{14}}{1.711 \times 10^{13}} = 52$$ for the Si BJT,

$$\beta = \frac{Q_E}{Q_B} = \frac{8.8929 \times 10^{14}}{0.76782 \times 10^{13}} = 115.82$$ for the SiGe BJT,

and

$$\beta = \frac{316.87 \times 10^{13}}{0.6362278 \times 10^{13}} = 498.04$$ for the InP BJT.

4. RESULTS AND DISCUSSION

4.1. DC Characteristics

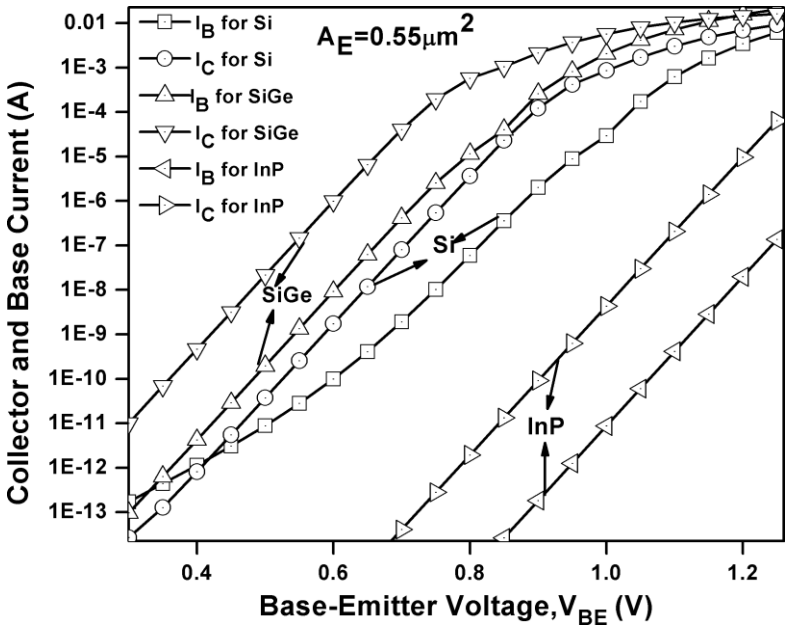

Figure 2. Total Gummel plot of all proposed devices.

The Gummel plots for the BJTs based on the three materials (Si, SiGe and InP) are shown in Figure 2. These plots indicate that the SiGe BJT has a superior performance (compared to the other two BJTs) in terms of the DC current gain when the base-emitter voltage is small (near about 0.3 V). However, at a higher base-emitter voltage (more than 1 V), the InP BJT shows better current gain compared to the Si and SiGe BJTs.

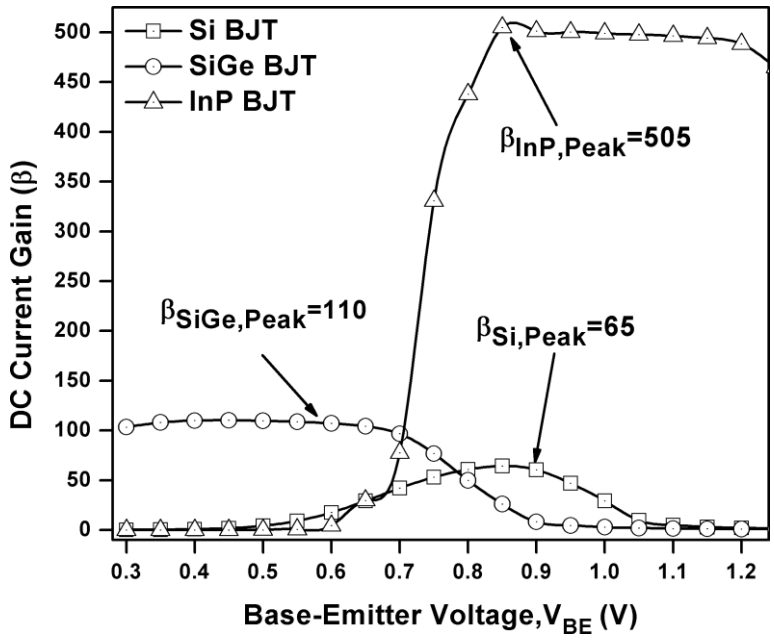

Figure 3. DC Current gain of all proposed devices.

The DC current gain (β) is plotted in Figure 3. The figure indicates maximum β of 505, 110 and 65 respectively for the InP, SiGe and Si BJTs against their theoretically calculated values of 498, 116, and 52 determined using Gummel-Poon model described in Section 3. The close agreements of the two values in each case justify the use of our simulation model. The high value of DC gain (β=505) in InP BJT is a clear advantage of the Gaussian doping profile against an extremely poor value (β=12) from a uniformly doped structure [4]. The high β in InP can be explained as follows. In order to have a good npn transistor, almost all electrons injected by the emitter into the base must be collected. Thus, the p-type base region should be narrow, and the electron lifetime τ_n should be long. This requirement is summed up by specifying $W_B << L_n$, where W_B is the length of the neutral base (measured between the depletion regions of the emitter and collector junctions) and L_n is the diffusion length for electrons in the base $(D_n\tau_n)^{1/2}$. Therefore, the InP BJT with the maximum diffusion length exhibits the highest β followed by the SiGe and Si BJT.

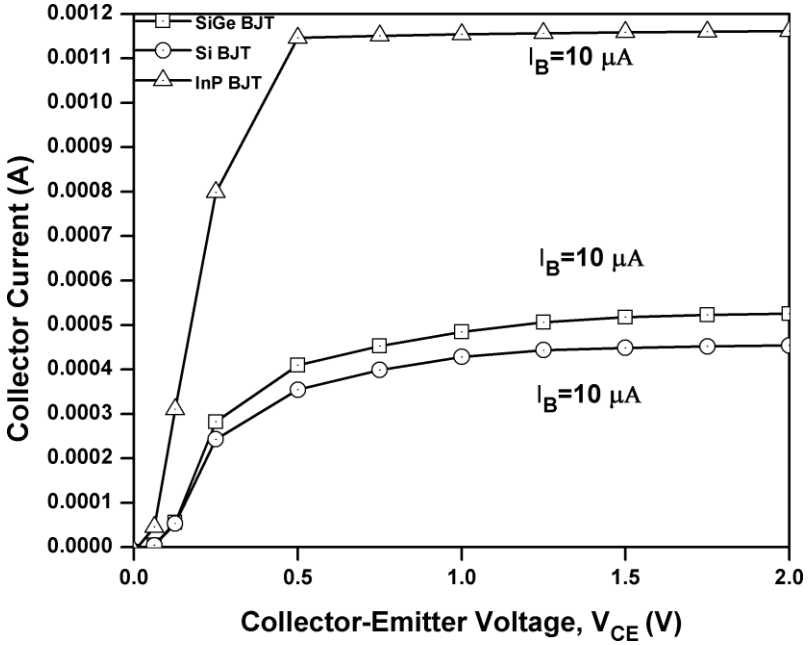

Figure 4. Common-emitter current-voltage characteristics.

The I_C versus V_{CE} curves are shown in Figure 4, which reveal a great deal of information on the physics behind the operation of the devices. These curves are plotted for I_B = 10 μA. The maximum collector current for the InP BJT is found to be about 1.15 mA while those for the SiGe and Si BJTs are recorded to be about 0.45 mA and 0.35 mA respectively. It is clear that for the same base current, InP based BJT provides more collector current than the Si and SiGe BJT which is proven by the highest β of InP BJT.

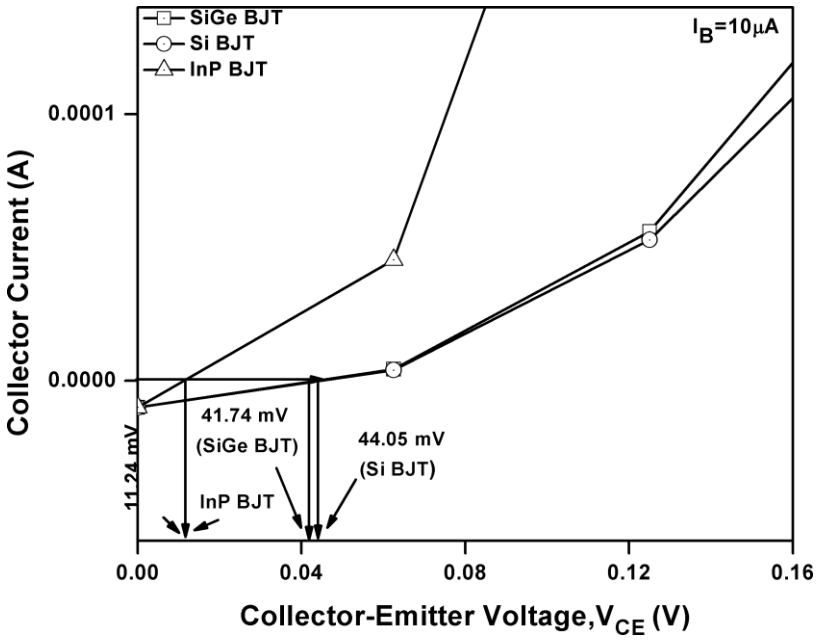

Figure 5. Offset voltage of all proposed devices.

The $V_{ce,offset}$ voltage is computed from the V_{CE}-I_C curve by expanding the output characteristics curve near the origin. The said voltage for Si, SiGe, and InP BJT are shown in Figure 5. The offset voltage is observed to be 11.24 mV, 41.74 mV and 44.05 mV, for the InP SiGe, and Si BJTs respectively. The offset voltage can be expressed as [9]:

$$\Delta V_{CE} = I_B R_E + \frac{KT}{q}\ln\left(\frac{A_C}{A_E}\right) + \frac{KT}{q}\ln\left(\frac{J_{CS}}{\alpha_N J_{ES}}\right) \tag{12}$$

Where R_E is the emitter series resistance, A_C and A_E are junction areas, and J_{CS} and J_{ES} are the reverse saturation current densities of the collector-base (CB) and emitter-base (EB) junctions respectively, and α_N is the forward base current gain. From the above expression in Equation (12), it is clear that InP BJT has a low offset voltage compared to the Si and SiGe BJT due to high mobility and high DC forward gain in the InP BJT. The high offset voltage observed in Si BJT may be attributed to high R_E and low DC forward current gain.

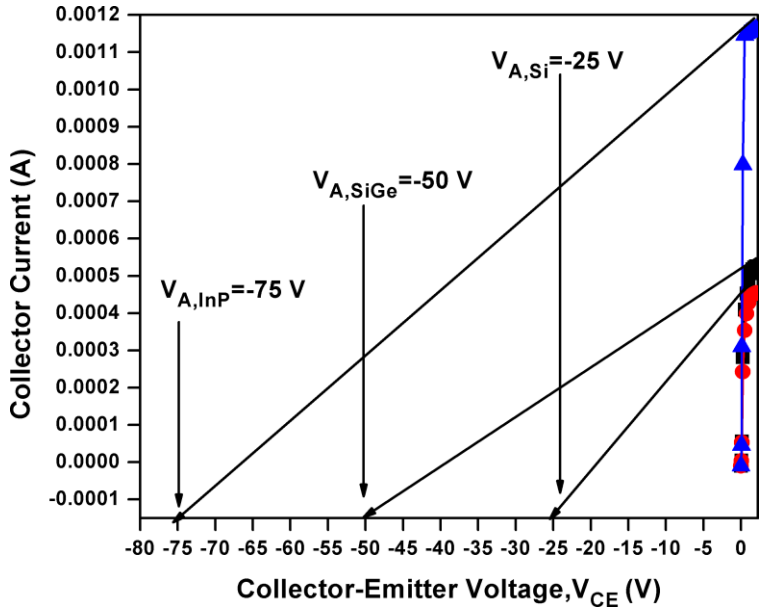

Figure 6. Early Voltage (V_A) of all devices.

The Early Voltage (V_A) is computed from backward extrapolated V_{CE}-I_C characteristics shown in Figure 6. The observed Early Voltages for Si, SiGe, and InP BJTs are -25 V, -50 V, and -75 V respectively. The V_A is a simple and convenient measure of the output conductance. Higher V_A is desirable for a BJT for better circuit operation. The V_A can be expressed as [10]:

$$V_A = \frac{\int_0^{W_B} N_{aB}(x)dx}{N_{aB}W_B\{\frac{\partial W_B}{\partial V_{CB}}\}} = \frac{Q_B(0)}{C_{CB}} \tag{13}$$

Where $Q_B(0)$ is the total base charge at V_{CB} = 0 V and C_{CB} is the collector base depletion capacitance.

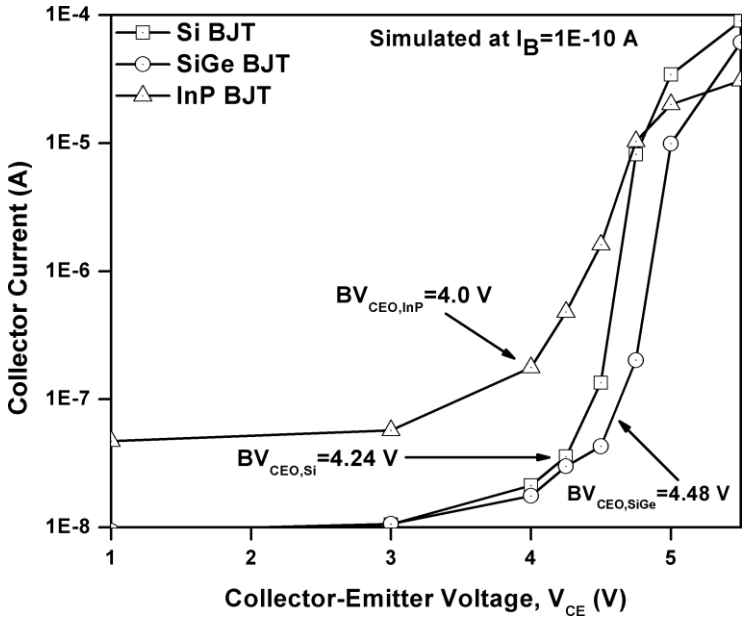

Figure 7. Breakdown voltage of all devices.

The breakdown voltages in the open base configuration, BV_{CEO} for Si, SiGe, and InP BJTs are shown in Figure 7. The three BJTs are simulated at a base current of, I_B=1e-10 A. The reason for choosing such a small base current is to assume that the base terminal is open. The observed breakdown voltages for the three BJTs are 4.24 V, 4.48 V, and 4 V respectively. The open base configuration BV_{CEO} can be expressed as [11]:

$$BV_{CEO} = \frac{BV_{CBO}}{\sqrt[n]{\beta}} \tag{14}$$

Where BV_{CBO} is the CB breakdown voltage with the emitter left open. The low breakdown voltage for InP BJT can be obtained from expression in Equation (14), that the high DC current gain of the device is mainly responsible for the same.

4.2. RF and Microwave Characteristics

The RF and Microwave characteristics of the device are studied by AC small-signal analysis using a two-port network [12]. The characteristics analyzed include cut-off frequency (f_t), maximum frequency of oscillation (f_{max}), Mason's Unilateral Gain (MUG), and stability factor. The input reflection coefficients of the devices are computed from the Smith Chart.

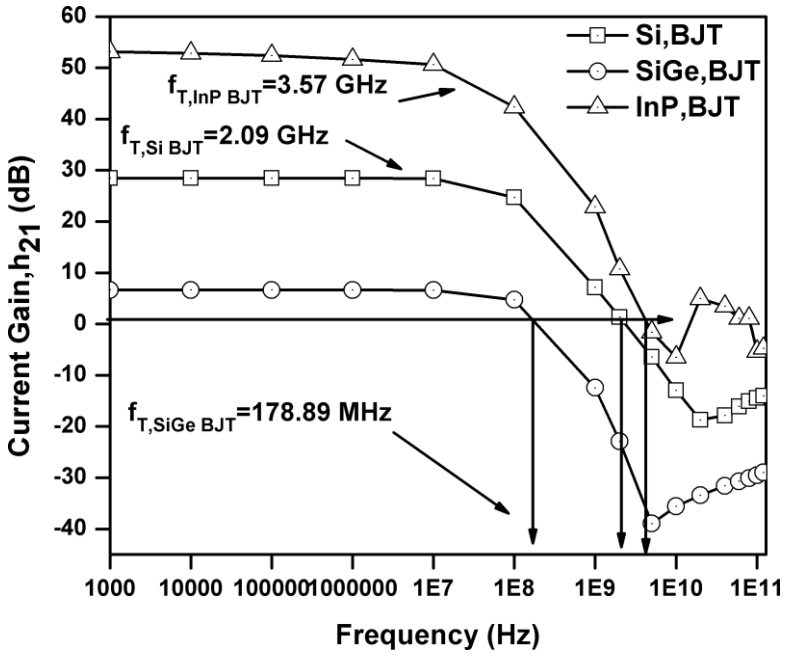

Figure 8. Cut-off frequency (f_t) of all devices.

The high-frequency performance of the simulated bipolar transistors is characterized by 'S' parameters extracted from the Silvaco tool. The cutoff frequency (f_t), defined as the frequency at which the magnitude of short circuit current gain $|h_{21}| = 1$, is plotted in Figure 8. They are recorded to be 2.09 GHz, 178.89 MHz, and 3.57 GHz for the Si, SiGe and InP BJTs respectively. The cut-off frequency (f_t) can be expressed as:

$$f_t = \frac{1}{2\pi\tau_b} \tag{15}$$

Where τ_b is the base transit time, defined as the time required to discharge the excess minority carriers in the base through the collector current [13]:

$$\tau_b = \frac{W_B^{\,2}}{D_{nB}} \tag{16}$$

Where, W_B^2 is the width of the base region, and D_{nB} is the diffusion coefficient of electrons in the base region. It is observed that the D_n values of InP, Si and SiGe are respectively 130cm^2/s, 36 cm^2/s, and 2.4 cm^2/s [14]. Thus, it is clear that InP has a high D_n compared to Si and SiGe. This makes the base transit-time small in InP BJT with the consequence of higher cutoff frequency of the device compared to the others.

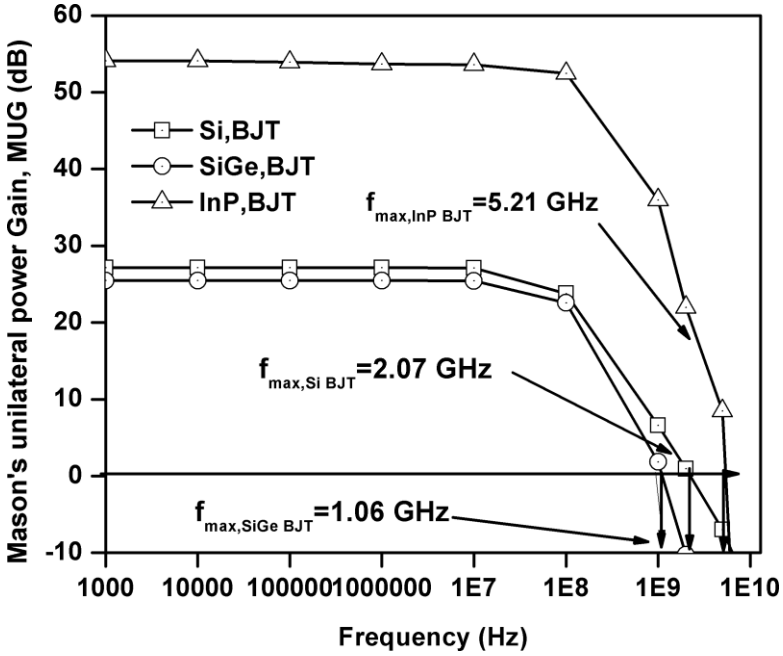

Figure 9. Maximum frequency of oscillation (f_{max}) of all devices.

f_{max} is the maximum oscillation frequency of a device and it is determined with the condition $|MUG| = 1$, using a unit-gain-point method. A comparative account of Massion's Unilateral Power Gain plots for all the transistors is presented in Figure 9. The maximum frequencies of oscillation f_{max} of Si, SiGe and InP based BJTs are found to be 2.07, 1.06 and 5.21 GHz respectively. The maximum oscillation frequency is expressed as [13]:

$$f_{max} = \sqrt{\frac{f_t}{8\pi r_b c_{jc}}} \tag{17}$$

Where f_t is cut-off frequency, r_b the base resistance, and c_{jc} is the collector junction capacitance. The transistor having reverse transmission parameter Y_{12} (or Z_{12}, h_{12}, S_{12}) as zero is called unilateral. The output is completely isolated from its input. Unilateral power gain U in terms of S parameters is expressed as [13]:

$$U = \frac{\left|\frac{S_{21}}{S_{12}} - 1\right|^2}{2K\left|\frac{S_{21}}{S_{12}}\right| - 2\mathrm{Re}\left(\frac{S_{21}}{S_{12}}\right)} \tag{18}$$

The stability factor, K, measures whether a transistor will be unconditionally stable for arbitrary passive loads [15]. The Rollett stability factor can be expressed in terms of S-parameters as [13]:

$$K = \frac{1 - \left|s_{11}\right|^2 - \left|s_{22}\right|^2 + \left|\Delta s\right|^2}{2\left|s_{12}.s_{21}\right|} \tag{19}$$

where, $\Delta s = s_{11}s_{22} - s_{12}s_{21}$.

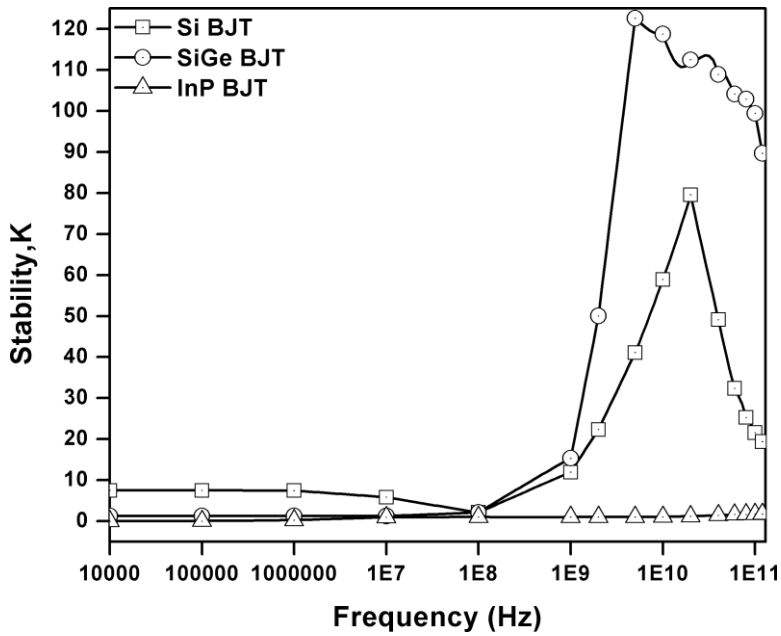

Figure 10. Stability (K) of all devices.

Figure 10 shows the stability factors of all the transistors. It is observed that the InP BJT is potentially unstable as K<1, whereas Si and SiGe BJTs are both inherently stable as K>1 for them.

The RF parameters S_{11} and S_{22} for the Si, SiGe, and InP BJTs are computed using Smith Chart in the frequency range from 1 Hz to 120 GHz. Smith Chart helps determine the device input and output reflection coefficients (Γ). If Γ is less than 0.33, then there is no need of any matching network at the input as well as output side. Mathematically, reflection coefficient at the input side is expressed as:

$$\Gamma_{in} = \sqrt{\mathrm{Re}(S_{11})^2 + \mathrm{Im}(S_{11})^2} \tag{20}$$

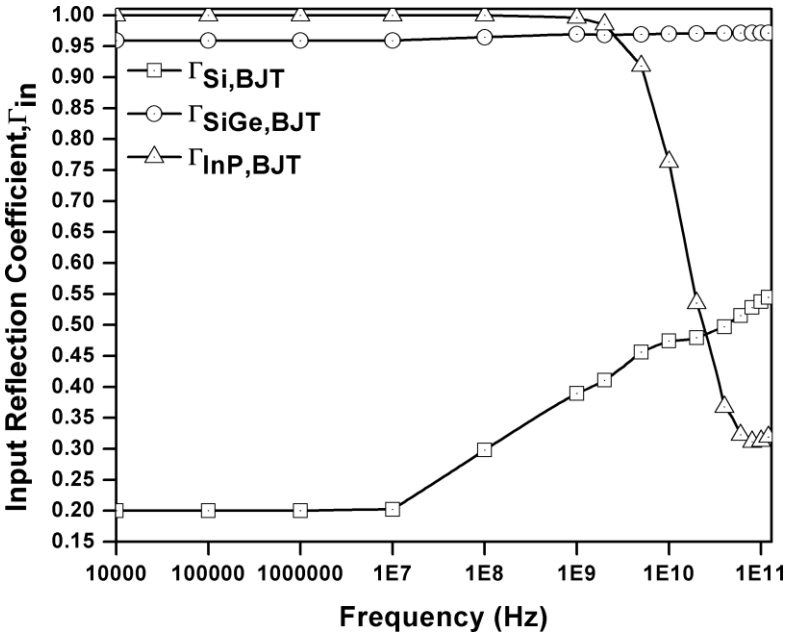

Figure 11. Input reflection coefficient (Γ) of all devices.

The reflection coefficient as a function of frequency is plotted in Figure 11. It is clear that the reflection coefficient, Γ_{in} < 0.33 for the Si BJT up to 100 MHz, which indicates that a matching network, at the input side, is not required. Above 100 MHz however, the reflection coefficient, Γ_{in} > 0.33, indicating that a matching network is necessary. For the SiGe BJT, the reflection coefficient, Γ_{in} > 0.33 throughout the frequency range. While the matching network is necessary for the SiGe BJT throughout the frequency range from 10 kHz to 100 GHz, the InP BJT requires matching network only up to 40 GHz.

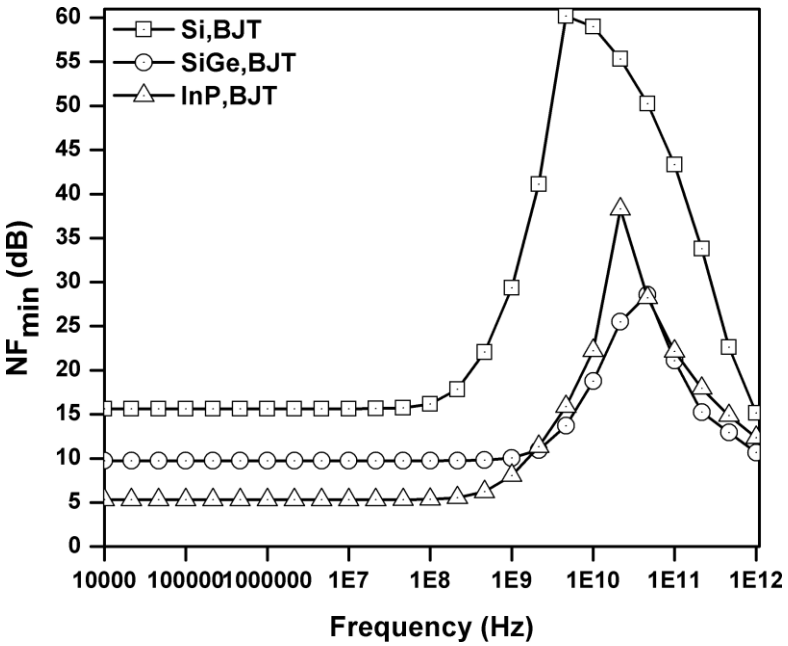

Figure 12. Minimum noise (NF_{min}) of all devices.

The minimum noise figures NF_{min} was determined by sweeping the base bias from 0 to 1.25 V and the collector bias from 0 to 2 V while keeping the emitter voltage zero. Thus, the NF_{min} determined for the Si, SiGe, and InP BJTs are depicted in Figure 12. Figure 12 shows that the NF_{min} records constant values of 5 dB, 10 dB, and 16 dB for the InP, SiGe, and Si BJTs respectively, up to a frequency of 0.1 GHz. Thereafter, the NF_{min} curves rise steeply to attain some peaks and then fall quickly to low values. Such behavior of NF_{min} can be understood by writing the theoretical expression as [10]:

$$NF_{\min} = 1 + \frac{1}{\beta} + \sqrt{2g_m r_b}\sqrt{\frac{1}{\beta} + \left(\frac{f}{f_T}\right)^2} \tag{21}$$

In Equation (21), the expression stated that NF_{min} depends on β and f_t in a critical way. At low frequency (lower than f_t), the second term inside the square root becomes negligible. Equation (21) is manifested in two ways. First, the frequency dependence of NF_{min} vanishes which renders it constant, and secondly the DC gain dominates as a reciprocal term, for which the constant values of NF_{min} are observed to be in the reverse order of β values for the three materials based BJTs.

5. CONCLUSION

Based on this study, we have compared, analyzed, and validated the different properties of the BJTs using TCAD Software and simple physics relations within this framework. The InP BJT is found to exhibit the highest current gain of 505, which is a potential advantage of a homojunction BJT because its fabrication process is less stringent compared to the HBT. The low offset voltage of InP BJT is preferable for digital application due to low power dissipation. In addition, the InP BJT has the highest V_A, f_t, and f_{max} among the three BJTs. On the other hand, Si, and SiGe BJTs have higher breakdown voltage and they are potentially stable compared to InP BJT.

REFERENCES

[1] Pierpaolo Palestri, Claudio Fiegna, Luca Selmi, Michael S. Peter, G. A. M. Hurkx, Jan W. Slotboom & Enrico Sangiorgi," A Better Insight into the Performance of Silicon BJT's Featuring Highly Nonuniform Collector Doping Profiles," IEEE Transactions on Electron Devices **47**, 5 (2000) 1044–1051.

[2] M. Jagadesh Kumar & Vijay S. Patri, "On the Iterative Schemes to Obtain Base Doping Profiles for Reducing Base Transit Time in a Bipolar transistor," IEEE Transactions on Electron Devices **48,** 6 (2001) 1222–1224.

[3] Gregory N. Henderson, Matthew F. O' Keefe, Timothy E. Boles, Paulette Noonan, John M. Sledziewski & Brian M. Brown, "SiGe Bipolar Junction Transistors for microwave power applications," IEEE MTT-S International Microwave Symposium Digest, (1997) 1299-1302.

[4] L. M. Su, N. Grote, F. Schmitt, "Diffuse planar InP Bipolar Junction Transistor with a Cadmium oxide film emitter," Electronics Letters **20**, 18 (1984) 716–717.

[5] I. M´artil, J. M. Marti, S. Garcıa, G. Gonzalez-Diaz, "Experimental Verification of the Physics and Structure of the Bipolar Junction Transistor," IEEE Transactions on Education **41**, 3 (1998) 224–228.

[6] Gananath Dash, Electronic Devices and Circuits, Universities Press, India, (2017).

[7] N. Rinaldi, "Analysis of the Depletion Layer of Exponentially Graded P–N Junctions with Nonuniformly Doped Substrates," IEEE Transactions on Electron Devices **47**, 12 (2000) 716-717.

[8] M. S. Tyagi, Introduction to Semiconductor Materials and Devices, John Wiley & Sons, UK, (1991).
[9] Jung-Hui Tsai, Yu-Jui Chu, "Influence of Spacer Layer on InP/InGaAs δ doped Heterojunction Bipolar Transistors," Materials Chemistry and Physics **91** (2004) 431–436.
[10] John D. Cressler, Guofu Niu, Silicon-Germanium Heterojunction Bipolar Transistors, Artech House, Boston, (2003).
[11] Donald A. Neaman, Semiconductor Physics and Devices, Tata McGraw-Hill Publishing, India, (2007).
[12] T. R. Lenka, G. N. Dash, A. K. Panda, "RF and Microwave Characteristics of a 10 nm thick InGaN-Channel Gate recessed HEMT," Journal of Semiconductors **34**, 11 (2013) 114003 (1-6).
[13] William Liu, Handbook of III-V Heterojunction Bipolar Transistors, John Wiley & Sons, UK, (1998).
[14] Web resource: *www.ioffe.ru/SVA/NSM/Semicond/*
[15] Steve C. Cripps, RF Power Amplifiers for Wireless Communications, Artech House, Boston, (2006).